J|A|C|S
ARTICLES
Published on Web 05/26/2007

Activation of Metal Hydride Complexes by Tri-*tert*-butylphosphine-Platinum and -Palladium Groups

Richard D. Adams,* Burjor Captain, Eszter Trufan, and Lei Zhu

Contribution from the Department of Chemistry and Biochemistry, University of South Carolina, Columbia, South Carolina 29208

Received January 27, 2007; E-mail: Adams@mail.chem.sc.edu

Abstract: The compounds $HM(CO)_4SnPh_3$, M = Os (**10**), Ru (**11**) are activated in the presence of $Pt(PBu^t_3)_2$ and $Pd(PBu^t_3)_2$ toward the insertion of PhC_2H into the M−H bond. The compounds $PtOs(CO)_4(SnPh_3)(PBu^t_3)[\mu\text{-HCC(H)Ph}]$, **12**, and $PtOs(CO)_4(SnPh_3)(PBu^t_3)[\mu\text{-H}_2\text{CCPh}]$, **13**, were obtained from the reaction of **10** with PhC_2H in the presence of $Pt(PBu^t_3)_2$. Compounds **12** and **13** are isomers containing alkenyl ligands formed by the insertion of the PhC_2H molecule into the Os−H bond at both the substituted and unsubstituted carbon atoms of the alkyne. Both compounds contain a $Pt(PBu^t_3)$ group that is bonded to the osmium atom and a bridging alkenyl ligand that is π-bonded to the osmium atom. The reaction of **11** with PhC_2H in the presence of $Pt(PBu^t_3)_2$ yielded the products $PtRu(CO)_4(SnPh_3)(PBu^t_3)[\mu\text{-HC}_2\text{(H)Ph}]$, **14**, and $PtRu(CO)_4(SnPh_3)(PBu^t_3)[\mu\text{-H}_2\text{C}_2\text{Ph}]$, **15**, which are also isomers similar to **12** and **13**. The reaction of **11** with PhC_2H in the presence of $Pd(PBu^t_3)_2$ yielded the product $PdRu(CO)_4(SnPh_3)(PBu^t_3)[\mu\text{-H}_2\text{C}_2\text{Ph}]$, **16**. Compound **16** contains a $Pd(PBu^t_3)$ group bonded to the ruthenium atom and a bridging H_2C_2Ph ligand that is π-bonded to the palladium atom. Compound **10** reacted with $Pt(PBu^t_3)_2$ in the absence of PhC_2H to yield the compound $PtOs(CO)_4(SnPh_3)(PBu^t_3)(\mu\text{-H})$, **17**. Compound **17** is a $Pt(PBu^t_3)$ adduct of **10**. It contains a Pt−Os bond with a bridging hydrido ligand. Compound **17** reacted with PhC_2H to yield **12**. Compound **12** reacted with PhC_2H to yield the compound $PtOs(CO)_3(SnPh_3)(PBu^t_3)[\mu\text{-HCC(Ph)C(H)C(H)Ph}]$, **18**. Compound **18** contains a bridging 2,4-diphenylbutadienyl ligand, HCC(Ph)C(H)C(H)Ph, that is π-bonded to the osmium atom and σ-bonded to the platinum atom. Fenkse−Hall molecular orbitals of **17** were calculated. The LUMO of **17** exhibits an empty orbital on the platinum atom that appears to be the most likely site for PhC_2H addition prior to its insertion into the Os−H bond.

Introduction

In recent studies we have demonstrated the synthesis of a variety of electronically unsaturated heteronuclear metal cluster complexes by the addition of $Pd(PBu^t_3)$ and $Pt(PBu^t_3)$ groups to the metal−metal bonds of transition metal carbonyl cluster complexes.[1−5] Some examples of these are the complexes $Ru_3Pd_3(CO)_{12}(PBu^t_3)_3$, **1**,[1a] $Ir_4Pt_2(CO)_{12}(PBu^t_3)_2$, **2**,[3] and $Rh_6Pt_4(CO)_{16}(PBu^t_3)_4$, **3**.[5] The electronic unsaturation is created both by the tendency of Pd and Pt to accommodate electron configurations that are less than 18 electrons/metal atom and also by the steric crowding produced by the PBu_3^t ligand which inhibits a normal complement of supporting ligands.

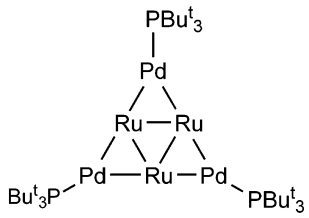

1

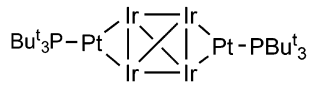

2

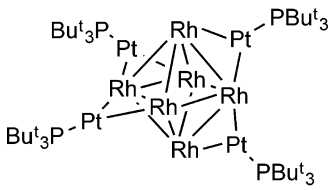

3

(1) (a) Adams, R. D.; Captain, B.; Fu, W.; Hall, M. B.; Manson, J.; Smith, M. D.; Webster, C. E. *J. Am. Chem. Soc.* **2004**, *126*, 5253−5267. (b) Adams, R. D.; Captain, B.; Fu, W.; Smith, M. D. *J. Am. Chem.* Soc. **2002**, *124*, 5628−5629. (c) Adams, R. D.; Captain, B.; Zhu, L. *Organometallics* **2006**, *45*, 430−436. (d) Adams, R. D.; Captain, B.; Zhu, L. *J. Cluster Sci.* **2006**, *17*, 87−95.

(2) (a) Adams, R. D.; Captain, B.; Fu, W.; Pellechia, P. J.; Smith, M. D. *Angew. Chem., Int. Ed.* **2002**, *41*, 1951−1953. (b) Adams, R. D.; Captain, B.; Fu, W.; Pellechia, P. J.; Smith, M. D. *Inorg. Chem.* **2003**, *42*, 2094−2101. (c) Adams, R. D.; Captain, B.; Fu, W.; Pellechia, P. J.; Zhu, L. *Inorg. Chem.* **2004**, *43*, 7243−7249.

(3) Adams, R. D.; Captain, B.; Hall, M. B.; Smith, J. L., Jr.; Webster, C. E. *J. Am. Chem. Soc.* **2005**, *127*, 1007−1014.

(4) (a) Adams, R. D.; Captain, B.; Herber, R. H.; Johansson, M.; Nowik, I.; Smith, J. L., Jr.; Smith, M. D. *Inorg. Chem.* **2005**, *44*, 6346−6358. (b) Adams, R. D.; Captain, B.; Zhu, L. *Organometallics* **2006**, *25*, 2049−2054.

(5) Adams, R. D.; Captain, B.; Pellechia, P. J.; Smith, J. L. *Inorg. Chem.* **2004**, *43*, 2695−2702.

Scheme 1[a]

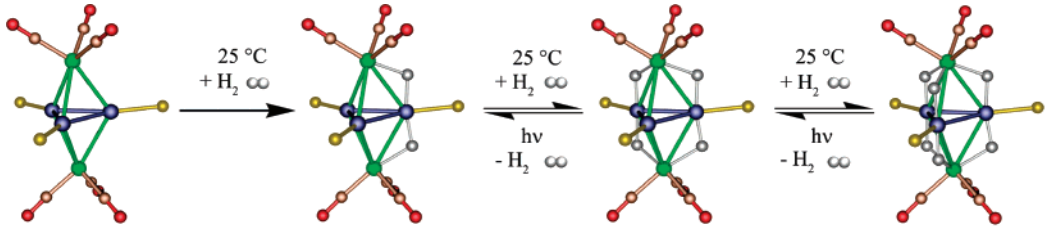

[a] Platinum (blue), rhenium (green), phosphorus (gold), oxygen (red), carbon (pink), hydrogen (gray).

Scheme 2[a]

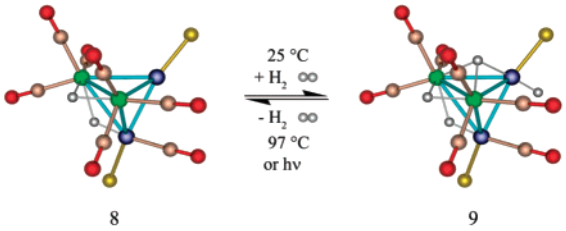

[a] Platinum (blue), rhenium (green), phosphorus (gold), oxygen (red), carbon (pink), hydrogen (gray).

We have also shown that the $Pt(PBu^t_3)$ group can be integrated into the architecture of the metal cluster to produce very highly unsaturated complexes that are capable of adding hydrogen under very mild conditions. In some cases, this is reversible.[6−7] For example, the 62 electron complex $Pt_3Re_2(CO)_6(PBu^t_3)_3$, **4**, sequentially adds 3 equiv of H_2 to form the compounds $Pt_3Re_2(CO)_6(PBu^t_3)_3(\mu\text{-}H)_2$, **5**, $Pt_3Re_2(CO)_6(PBu^t_3)_3(\mu\text{-}H)_4$, **6**, and $Pt_3Re_2(CO)_6(PBu^t_3)_3(\mu\text{-}H)_6$, **7**, Scheme 1.[6a] Some of the hydrogen is released from these hydride complexes when they are irradiated with UV−vis radiation.

Another example is the unsaturated dirheniumdiplatinum complex $Pt_2Re_2(CO)_7(PBu^t_3)_2(\mu\text{-}H)_2$, **8**, that adds 1 equiv of H_2 at room temperature to yield the tetrahydrido complex $Pt_2Re_2(CO)_7(PBu^t_3)_2(\mu\text{-}H)_4$, **9**, Scheme 2.[7] The hydrogen addition to **8** can be reversed by both thermal and photochemical means; see Scheme 2.

The adsorption and activation of hydrogen will be important both to the storage and the utilization of hydrogen in energy systems of the future.[8]

We have now found that $Pd(PBu^t_3)_2$ and $Pt(PBu^t_3)_2$ can activate hydride containing metal carbonyl complexes toward insertion of alkynes into a metal−hydrogen bond by generating a $M(PBu^t_3)$, M = Pd or Pt, group that interacts with the hydrido ligand in the complex prior to the addition/insertion of the alkyne into the metal−hydrogen bond. In this first report, we describe the results of our studies of the insertion of the alkyne, phenylacetylene, PhC_2H, into the M−H bonds of the compounds $HM(CO)_4SnPh_3$, M = Os (**10**), Ru (**11**). The insertion of alkynes and alkenes into a metal−hydrogen bond is one of the most basic steps in the process of catalytic hydrogenation through which alkynes are converted to alkenes and alkenes are converted to alkanes.[9] In general, these reactions proceed by the coordination of a substrate to a metal atom prior to a C−H bond forming insertion step.[9b] A preliminary report of a portion of this work has recently been published.[10]

Experimental Section

General Data. All the reactions were performed under a nitrogen atmosphere using the standard Schlenk techniques. Reagent grade solvents were dried by the standard procedures and were freshly distilled prior to use. Infrared spectra were recorded on an AVATAR 360 FT-IR spectrophotometer. ^{1}H NMR and ^{31}P NMR were recorded on a Varian Mercury 400 spectrometer operating at 399 and 162 MHz, respectively. ^{31}P NMR spectra were externally referenced against 85% *ortho*-H_3PO_4. Variable temperature ^{1}H NMR and ^{31}P NMR spectra were recorded on a Varian Inova 500 operating at 500.2 and 202.5 MHz, respectively. Elemental analyses were performed by Desert Analytics (Tucson, AZ). Mass spectrometric measurements performed by a direct exposure probe using electron impact ionization (EI) were made on a VG 70S instrument. Triphenylstannane (Ph_3SnH) and phenylacetylene (PhC_2H) were purchased from Aldrich and were used without further purification. $Ru_3(CO)_{12}$, $Pd(PBu^t_3)_2$, and $Pt(PBu^t_3)_2$ were purchased from STREM and were used without further purification. $HOs(CO)_4SnPh_3$, **10**, was prepared according to the previously published procedure.[11] Product separations were performed by TLC in air on Analtech 0.25 mm silica gel 60 Å F254 glass plates.

Synthesis of $HRu(CO)_4SnPh_3$, 11. A solution of $Ru(CO)_5$ was prepared and used *in situ* as follows.[12] A 40 mg amount of $Ru_3(CO)_{12}$ (0.063 mmol) was dissolved in 120 mL of hexane in a 250 mL Pyrex three-neck flask. The solution was placed in an ice bath and irradiated using a medium-pressure mercury UV lamp (1000 W) in the presence of a slow purge of carbon monoxide (CO) for approximately 25 min. During this time the orange colored solution turned colorless. The reaction flask was then evacuated and refilled with nitrogen to remove the excess CO. A 79 mg amount of $HSnPh_3$ (0.225 mmol) was then added to the $Ru(CO)_5$ solution at 0 °C. The solution was then heated to reflux for 10 min during which time the colorless solution turned

(6) (a) Adams, R. D.; Captain, B.; Beddie, C.; Hall, M. B. *J. Am. Chem. Soc.* **2007**, *129*, 986−1000. (b) Adams, R. D.; Captain, B. *Angew. Chem., Int. Ed.* **2005**, *44*, 2531−2533.
(7) (a) Adams, R. D.; Captain, B.; Smith, M. D.; Beddie, C. L.; Hall, M. B. *J. Am. Chem. Soc.* **2007**, *129*, 5981−5991. (b) Adams, R. D.; Captain, B.; Smith, M. D. *Angew. Chem., Int. Ed.* **2006**, *45*, 1109−1112.
(8) (a) Crabtree, G. W.; Dresselhaus, M. S.; Buchanan, M. V. The Hydrogen Economy. *Physics Today* **2004**, 39−44. (b) Ogden, J. M. Hydrogen: The Fuel of the Future? *Physics Today* **2002**, *55*, 69−75. (c) Schlapbach, L.; Züttel, A. *Nature* **2001**, *414*, 353−358. (d) Zecchina, A.; Borgida, S.; Vitillo, J. G.; Ricchiardi, G.; Lamberti, C.; Spoto, G.; Bjørgen, M.; Lillerud, K. P. *J. Am. Chem. Soc.* **2005**, *127*, 6361−6366. (e) Nijkamp, M. G.; Raaymakers, J. E. M. J.; van Dillen, A. J.; de Jong, K. P. *Appl. Phys. A* **2001**, *72*, 619−623. (f) Weitkamp, J.; Fritz, M.; Ernst, S. *Int. J. Hydrogen Energy* **1995**, *20*, 967−970. (g) Rosi, N. L.; Eckert, J.; Eddaoudi, M.; Vodak, D. T.; O'Keerre, M.; Yaghi, O. M. *Science* **2003**, *300*, 1127−1129. (h) Zhao, X.; Xiao, B.; Fletcher, A. J.; Thomas, K. M.; Bradshaw, D.; Rosseinsky, M. J. *Science* **2004**, *306*, 1012−1015. (i) Rowsell, J. L. C.; Eckert, J.; Yaghi, O. M. *J. Am. Chem. Soc.* **2005**, *127*, 14904−14099. (j) Dinca, M.; Long, J. R. *J. Am. Chem. Soc.* **2005**, *127*, 9376−9377. (k) Kaye, S. S.; Long, J. R. *J. Am. Chem. Soc.* **2005**, *127*, 6506−6507. (l) Sun, D.; Ma, S.; Ke, Y.; Collins, D. J.; Zhou, H.-C. *J. Am. Chem. Soc.* **2006**, *128*, 3896−3897.
(9) (a) Selmeczy, A. D.; Jones, W. D. *Inorg. Chim. Acta* **2000**, *300*−*302*, 138. (b) Collman, J. P.; Hegedus, L. S.; Norton, J. R.; Finke, R. G. *Principles and Applications of Organotransition Metal Chemistry*; University Science Books: Mill Valley, CA, 1987; Chapter 10.
(10) Adams, R. D.; Captain, B.; Zhu, L. *J. Am. Chem. Soc.* **2006**, *128*, 13672−13673.
(11) Adams, R. D.; Captain, B.; Zhu, L. *Organometallics* **2006**, *25*, 4183−4187.
(12) Huq, R.; Poë, A. J.; Chawla, S. *Inorg. Chim. Acta* **1980**, *38*, 121−125.

bright yellow. After cooling, the solvent was removed in vacuo, and the product was separated by TLC by using a 6:1 hexane−methylene chloride solvent mixture to yield 52 mg (49%) of light yellow **11**. NOTE: The TLC separation should be performed quickly as HRu(CO)$_4$SnPh$_3$ decomposes on silica gel. Spectral data for **11**: IR ν_{CO} (cm^{-1} in CH_2Cl_2): 2120 (m), 2060 (m, sh), 2037 (vs). ^{1}H NMR ($CDCl_3$, in ppm): $\delta = 7.30 - 7.57$ (m, 15 H, Ph), −7.66 (s, 1H, hydride, $^2J_{119_{Sn-H}} = 51$ Hz, $^2J_{117_{Sn-H}} = 49$ Hz). Elemental Anal. Calcd: C, 46.84; H, 2.86. Found: C, 46.99; H, 3.05%.

Preparation of PtOs(CO)$_4$(SnPh$_3$)(PBu$^t_3$)[μ-HCC(H)Ph], 12, and PtOs(CO)$_4$(SnPh$_3$)(PBu$^t_3$)[μ-H$_2$CCPh], 13. A 12.6 mg amount of **10** (0.020 mmol) and 14.2 mg amount of Pt(PBu$^t_3$)$_2$ (0.024 mmol) were dissolved in 10 mL of CH_2Cl_2 in a 25 mL three-neck flask, and 2.6 μL of phenylacetylene (0.024 mmol) was added by using a 10 μL microsyringe. The solution was stirred at room temperature for 10 min. The solvent was then removed in vacuo, and the product was separated by TLC by using hexane solvent to yield 7.0 mg (31%) of PtOs(CO)$_4$(SnPh$_3$)(PBu$^t_3$)[μ-HCC(H)Ph], **12**, and 4.4 mg (19%) of PtOs(CO)$_4$(SnPh$_3$)(PBu$^t_3$)[μ-H$_2$CCPh], **13**. Spectral data for **12**: IR ν_{CO} (cm^{-1} in CH_2Cl_2): 2049 (m), 2015 (m), 1977 (s); ^{1}H NMR (toluene-d_8 in ppm) at − 65 °C: $\delta = 9.25$ (d, 1H, CH, $^3J_{H-H} = 14$ Hz), 9.01 (d, 2H, CH, $^3J_{H-H} = 13$ Hz), 8.89 (d, 1H, CH, $^3J_{H-H} = 13$ Hz, $^3J_{Pt-H} = 51$ Hz), 6.02 (d, 1H, CH, $^3J_{H-H} = 13$ Hz), 5.87 (d, 1H, CH, $^3J_{H-H} = 13$ Hz), 5.73 (d, 1H, CH, $^3J_{H-H} = 13$ Hz), 4.82 (d, 1H, CH, $^3J_{H-H} = 14$ Hz); at +60 °C: $\delta = 1.12$ (d, 27H, CH_3, $^3J_{P-H} = 13$ Hz). ^{31}P{^{1}H} NMR (toluene-d_8 in ppm) at −50 °C: $\delta = 93.0$ (s, 1P, $^1J_{Pt-P} = 2952$ Hz), 90.8 (s, 1P, $^1J_{Pt-P} = 2942$ Hz, $^3J_{Sn-P} = 39$ Hz), 90.1 (s, 1P, $^1J_{Pt-P} = 3226$ Hz, $^3J_{Sn-P} = 20$ Hz), 88.0 (s, 1P, $^1J_{Pt-P} = 2910$ Hz, $^3J_{Sn-P} = 20$ Hz). Spectral data for **13**: IR ν_{CO} (cm^{-1} in CH_2Cl_2): 2060 (m), 2013 (m), 1980 (s); ^{1}H NMR (CD_2Cl_2 in ppm): $\delta = 4.82$ (d, 1H, CH, $^3J_{H-H} = 1.6$ Hz, $^3J_{Pt-H} = 135$ Hz, $^3J_{Sn-H} = 26$ Hz), 2.81 (dd, 1H, CH, $^2J_{H-H} = 1.6$ Hz, $^4J_{P-H} = 1.6$ Hz). ^{31}P{^{1}H} NMR (CD_2Cl_2 in ppm): $\delta = 98.5$ (s, 1P, $^1J_{Pt-P} = 3046$ Hz). Anal. Calcd: C, 43.75; H, 4.25. Found: C, 43.58; H, 4.12%.

Reaction of 11 with Pt(PBu$^t_3$)$_2$. Synthesis of PtRu(CO)$_4$(SnPh$_3$)(PBu$^t_3$)[μ-HCC(H)Ph], 14, and PtRu(CO)$_4$(SnPh$_3$)(PBu$^t_3$)[μ-H$_2$CCPh], 15. A 21.3 mg amount of Pt(PBu$^t_3$)$_2$ (0.035 mmol) was dissolved in 30 mL of CH_2Cl_2 in a 100 mL three-neck flask. Phenylacetylene (0.025 mL, 0.225 mmol) was added to the solution, and it was then heated to reflux for 20 min. To the refluxing solution, 20 mg of HRu(CO)$_4$(SnPh$_3$) (0.035 mmol) were added and stirred at reflux for another 10 min. The reaction mixture was then cooled, and the solvent and the excess phenylacetylene were removed in vacuo. The products were separated by TLC using a 6:1 hexane/methylene chloride solvent mixture to yield in order of elution: 2.0 mg (5%) of yellow PtRu(CO)$_4$(SnPh$_3$)(PBu$^t_3$)[μ-H$_2$CCPh], **15**, and 12.6 mg (33%) of light yellow PtRu(CO)$_4$(SnPh$_3$)(PBu$^t_3$)[μ-HCC(H)Ph], **14**. Spectral data for **14**: IR ν_{CO} (cm^{-1} in CH_2Cl_2): 2047 (s), 2014 (vs), 1972 (vs). ^{1}H NMR (toluene-d_8, in ppm) at 25 °C: $\delta = 9.29$ (d, 1H, CH, $^3J_{H-H} = 14$ Hz, isomer 1), 9.17 (broad, 1H, CH, isomer 2), 6.82 − 8.00 (m, 15H, Ph), 5.94 (broad, 1H, CH, isomer 2), 5.70 (broad, 1H, CH, isomer 1), 1.10 (d, CH_3, $^3J_{P-H} = 13$ Hz). ^{31}P {^{1}H} NMR ($CDCl_3$, in ppm) at 25 °C: $\delta = 100.0$ (s, 1P, $^1J_{Pt-P} = 2887$ Hz). ^{1}H NMR (toluene-d_8, in ppm) at −40 °C: 9.30 (d, 1H, CH, $^3J_{H-H} = 14$ Hz, isomer 1), 9.16 (d, 1H, CH, $^3J_{H-H} = 14$ Hz, isomer 2), 5.94 (d, 1H, CH, $^3J_{H-H} = 14$ Hz, isomer 2), 5.83 (d, 1H, CH, $^3J_{H-H} = 14$ Hz, isomer 1). Elemental Anal. Calcd **14**·1.5C_6H_6: C, 51.87; H, 4.95. Found: C, 51.49; H, 4.60%. Spectral data for **15**: IR ν_{CO} (cm^{-1} in CH_2Cl_2): 2058 (m), 2009 (s), 1988 (vs). ^{1}H NMR ($CDCl_3$, in ppm): $\delta = 7.10-7.74$ (m, 15 H, Ph), 4.51 (br, 1H, CH, $^3J_{Pt-H} = 129$ Hz, $^3J_{Sn-H} = 24$ Hz), 2.80 (dd, 1H, CH, $^4J_{P-H} = 2.9$ Hz, $^2J_{H-H} = 1.4$ Hz), 1.30 (d, CH_3, $^3J_{P-H} = 13$ Hz). ^{31}P {^{1}H} NMR ($CDCl_3$, in ppm): $\delta = 137.5$ (s, 1P, $^1J_{Pt-P} = 3158$ Hz, $^3J_{Sn-P} = 75$ Hz). The resonance at 4.51 ppm appears as a broad singlet due to coupling to ^{31}P and ^{1}H. The ^{13}P decoupled ^{1}H NMR spectrum resolved this resonance to a doublet with $^2J_{H-H} = 1.4$ Hz. The respective couplings of $^4J_{P-H} = 2.9$ Hz and $^2J_{H-H} = 1.4$ Hz for the resonance at 2.80 ppm were assigned based on the ^{31}P decoupled ^{1}H NMR spectrum. Elemental Anal. Calcd for **15**: C, 47.43; H, 4.64. Found: C, 48.60; H, 4.46%.

Synthesis of PdRu(CO)$_4$(SnPh$_3$)(PBu$^t_3$)[μ-H$_2$CCPh], 16. A 16 mg amount of Pd(PBu$^t_3$)$_2$ (0.031 mmol) was dissolved in 30 mL of CH_2Cl_2 in a 100 mL three-neck flask. Phenylacetylene (0.025 mL, 0.225 mmol) was added to the solution, and it was then heated to reflux for 20 min. To the refluxing solution, 20 mg of HRu(CO)$_4$(SnPh$_3$) (0.035 mmol) were added and stirred at reflux for another 10 min. The reaction mixture was then cooled, and the solvent and the excess phenylacetylene were removed in vacuo. The product was separated by TLC by using a 6:1 hexane/methylene chloride solvent mixture to yield 5.0 mg (15%) of yellow PdRu(CO)$_4$(SnPh$_3$)(PBu$^t_3$)[μ-H$_2$CCPh], **16**. Spectral data for **16**: IR ν_{CO} (cm^{-1} in CH_2Cl_2): 2078 (m), 2004 (vs), 1870 (w). ^{1}H NMR ($CDCl_3$, in ppm): $\delta = 7.20-7.70$ (m, Ph), 6.87−6.93 (m, Ph), 6.55−6.58 (m, Ph), 5.53 (dd, 1H, CH, $^3J_{P-H} = 2$ Hz, $^2J_{H-H} = 2$ Hz), 4.42 (d, 1H, CH, $^2J_{H-H} = 2$ Hz), 1.40 (d, CH_3, $^3J_{P-H} = 13$ Hz). The resonance at 5.53 appears as a triplet, but it is actually an overlapping doublet of doublets. The ^{31}P decoupled ^{1}H NMR spectrum showed a doublet for the resonance at 5.53 ppm indicating that this peak is coupled to both ^{31}P and ^{1}H, while the resonance at 4.42 ppm remained a doublet indicating that this resonance is coupled only to ^{1}H. ^{31}P {^{1}H} NMR ($CDCl_3$, in ppm): $\delta = 90.2$ (s, 1P, $^3J_{Sn-P} = 76$ Hz). Elemental Anal. Calcd for **16**: C, 51.64; H, 5.02. Found: C, 52.02; H, 5.23%.

Preparation of PtOs(CO)$_4$(SnPh$_3$)(PBu$^t_3$)(μ-H), 17. A 27 mg amount of **10** (0.042 mmol) was dissolved in 10 mL CH_2Cl_2 in a 50 mL three-neck flask. A 32 mg amount of Pt(PBu$^t_3$)$_2$ (0.053 mmol) was added, and the reaction stirred at room temperature for 25 min. The solvent was then removed in vacuo, and the product was purified by TLC by using 6:1 hexane−methylene chloride solvent mixture to yield 18.2 mg (45%) of PtOs(CO)$_4$(SnPh$_3$)(PBu$^t_3$)(μ-H), **17**. Spectral data for **17**: IR ν_{CO} (cm^{-1} in CH_2Cl_2): 2124 (w), 2076 (vs), 2038 (w, sh), 2010 (vs), 1809 (m). ^{1}H NMR (CD_2Cl_2 in ppm): $\delta = 1.34$ (d, 27H, CH_3, $^3J_{P-H} = 13$ Hz), −5.99 (d, H, hydride, $^2J_{P-H} = 46$ Hz, $^1J_{Pt-H} = 566$ Hz, $^2J_{119_{Sn-H}} = 46$ Hz, $^2J_{117_{Sn-H}} = 44$ Hz). ^{31}P{^{1}H} NMR (CD_2Cl_2 in ppm): $\delta = 101.8$ (s, 1P, $^1J_{Pt-P} = 6437$ Hz). Elemental Anal. Calcd for **17**: C, 38.86; H, 4.10. Found: C, 38.96; H, 4.14%.

Addition of PhC$_2$H to 17. A 14.8 mg amount of **17** (0.014 mmol) was dissolved in 10 mL of CH_2Cl_2 in a 50 mL three-neck flask. A 1.7 μL amount of PhC$_2$H (0.014 mmol) was added, and the reaction solution was stirred at room temperature for 15 min. The solvent was removed *in vacuo*, and the products were separated by TLC by using hexane solvent to elute. This yielded 4.5 mg (28% yield) of **12** and 2.7 mg (17% yield) of **13**.

Preparation of PtOs(CO)$_3$(SnPh$_3$)(PBu$^t_3$)[μ-HCC(Ph)C(H)C(H)Ph], 18. A 9.0 mg amount of **12** (0.0078 mmol) was dissolved in 10 mL of CH_2Cl_2 solvent in a 50 mL three-neck flask. A 10 μL amount of PhC$_2$H (0.094 mmol) was added, and the solution was heated to reflux for 60 min. The solvent was removed *in vacuo*, and the product was purified by TLC using a 6:1 hexane/methylene chloride solvent mixture to yield 4.7 mg (48%) of PtOs(CO)$_3$(SnPh$_3$)(PBu$^t_3$)[μ-HCC(Ph)C(H)C(H)Ph], **18**. Spectral data for **18**: IR ν_{CO} (cm^{-1} in CH_2Cl_2): 2020 (vs), 1980 (s), 1933 (m). ^{1}H NMR (in CD_2Cl_2): $\delta = 1.34$ (d, 27H, CH_3, $^3J_{P-H} = 13$ Hz), 8.85, (s, 1H, CH, $^2J_{Pt-H} = 33$ Hz), 7.13−7.39 (m, 25H, Ph), 6.87 (d, 1H, CH, $^3J_{H-H} = 9.8$ Hz), 4.92 (d, 1H, CH, $^3J_{H-H} = 9.8$ Hz). ^{31}P{^{1}H} NMR (in CD_2Cl_2): $\delta = 98.5$ (s, 1P, $^1J_{Pt-P} = 3045$ Hz, $^3J_{Sn-P} = 27$ Hz). Mass Spectrum: EI-MS showed the parent ion at *m*/*z* 1226.

Crystallographic Analysis. Orange crystals of **11** suitable for diffraction analysis were grown from solutions in hexane solvent under nitrogen by cooling to −80 °C. Colorless crystals of **12** suitable for diffraction analysis were grown by slow evaporation of solvent from a CH_2Cl_2/hexane solution at room temperature. Light yellow crystals of **13** and **18** suitable for diffraction analysis were grown by slow evaporation of solvent from solutions in CH_2Cl_2/hexane solvent mixtures at −20 °C. Yellow crystals of **14** suitable for diffraction analysis were grown by slow evaporation of solvent from a solution in a benzene/

Table 1. Crystallographic Data for Compounds **11**, **12**, and **13**

compound	**11**	**12**	**13**
empirical formula	$RuSnO_4C_{22}H_{16}$	$Pt_2Os_2P_2O_8C_{84}H_{98}$	$PtOsPO_4C_{42}H_{49}$
formula weight	564.11	2305.52	1152.76
crystal system	triclinic	triclinic	triclinic
lattice parameters			
a (Å)	9.6568(5)	15.2610(15)	10.3198(4)
b (Å)	10.8775(5)	15.4146(15)	12.1676(5)
c (Å)	11.3053(6)	21.044(2)	18.4225(8)
α (deg)	67.830(1)	76.544(2)	78.148(1)
β (deg)	89.132(1)	73.541(2)	78.187(1)
γ (deg)	83.812(1)	76.415(2)	65.989(1)
V (Å^3)	1092.91(10)	4540.8(8)	2048.97(15)
space group	$P\bar{1}$ (#2)	$P\bar{1}$ (#2)	$P\bar{1}$ (#2)
Z value	2	2	2
ρ_{calcd} (g/cm^3)	1.714	1.686	1.868
μ (Mo Kα) (mm^{-1})	1.856	6.480	7.181
temperature (K)	294(2)	294(2)	294(2)
$2\Theta_{max}$ (deg)	56.6	56.6	56.8
no. obsd ($I > 2\sigma(I)$)	4327	16059	16059
no. parameters	257	935	468
goodness of fit GOF[a]	1.047	1.051	1.031
max shift in cycle	0.001	0.002	0.002
residuals:[a] R1, wR2	0.0304, 0.0686	0.0405, 0.1230	0.0270, 0.0628
absorption correction, max/min	multi-scan 1.000/0.837	multi-scan 1.000/0.430	multi-scan 1.000/0.430
largest peak in final diff map (e$^-$/Å^3)	0.795	3.731	1.646

[a] $R = \Sigma_{hkl}(||F_{obsd}| - |F_{calcd}||)/\Sigma_{hkl}|F_{obsd}|$; $R_w = [\Sigma_{hkl}w(|F_{obsd}| - |F_{calcd}|)^2/\Sigma_{hkl}wF_{obsd}^2]^{1/2}$, $w = 1/\sigma^2(F_{obsd})$; GOF $= [\Sigma_{hkl}w(|F_{obsd}| - |F_{calcd}|)^2/(n_{data} - n_{vari})]^{1/2}$.

octane solvent mixture at 8 °C. Yellow crystals of **15**, orange crystals of **16**, and light yellow crystals of **17**, suitable for diffraction analysis, were grown by slow evaporation of solvent from solutions in CH_2Cl_2/hexane solvent mixtures at 8 °C. Each data crystal was glued onto the end of a thin glass fiber. X-ray intensity data were measured by using a Bruker SMART APEX CCD-based diffractometer using Mo Kα radiation ($\lambda = 0.710\ 73$ Å). The raw data frames were integrated with the SAINT+ program by using a narrow-frame integration algorithm.[13] Correction for the Lorentz and polarization effects were also applied by SAINT. An empirical absorption correction based on the multiple measurement of equivalent reflections was applied by using the program SADABS. All three structures were solved by a combination of direct methods and difference Fourier syntheses and refined by full matrix least-squares on F^2, by using the SHELXTL software package.[14] Crystal data, data collection parameters, and results of the analyses for compounds **11**−**18** are listed in Tables 1−3.

Compounds **11**−**16** and **18** all crystallized in the triclinic crystal system. The space group $P\bar{1}$ was assumed and confirmed in each case by the successful solution and refinement of the structure. All non-hydrogen atoms were refined with anisotropic thermal parameters. Hydrogen atoms on the *tert*-butyl groups and phenyl groups were placed in geometrically idealized positions and refined as standard riding atoms. The hydrogen atoms on the phenylacetylene ligand in all compounds were located in difference Fourier maps and were refined with isotropic thermal parameters. The hydride ligand in compound **11** was located in a difference Fourier map and was refined satisfactorily with an isotropic thermal parameter. For compound **12** there are two formula equivalents of the molecule in the asymmetric unit. For compound **14** one and a half solvent molecules of benzene cocrystallized with the complex. The solvent molecule was refined with isotropic thermal parameters.

Compound **17** crystallized in the monoclinic crystal system. The space group $P2_1/n$ was confirmed on the basis of the systematic absences in the data. The hydrido ligand was located and refined with a fixed isotropic thermal parameter. All non-hydrogen atoms were refined with anisotropic thermal parameters. Hydrogen atoms on the *tert*-butyl groups were placed in geometrically idealized positions and included as standard riding atoms.

Molecular Orbital Calculations. All molecular orbital calculations reported herein were performed by using the Fenske−Hall method.[15] The calculations were performed utilizing a graphical user interface developed[16] to build inputs and view outputs from stand-alone Fenske−Hall and MOPLOT2 binary executables.[17] Contracted double-ζ basis sets were used for the Os 5d, Pt 5d, Sn 5p, P 3p, and C and O 2p atomic orbitals. Hydrogen was used in place of both phenyl and *tert*-butyl groups in these calculations. The Fenske−Hall scheme is a nonempirical approximate method that is capable of calculating molecular orbitals for very large transition metal systems and has built-in fragment analysis routines that allow one to assemble transition metal cluster structures from ligand-containing fragments.

Results and Discussion

No reaction was observed when a solution of **10** and PhC_2H was heated to reflux in toluene solvent for a period of 1 h. However, when $Pt(PBu^t_3)_2$ was added to a similar solution of **10** and PhC_2H in CH_2Cl_2 solvent, a rapid reaction occurred at room temperature. Two products $PtOs(CO)_4(SnPh_3)(PBu^t_3)[\mu$-$HCC(H)Ph]$, **12**, and $PtOs(CO)_4(SnPh_3)(PBu^t_3)[\mu$-$H_2CCPh]$, **13**, were obtained and isolated in 31% and 19% yields, respectively. Both compounds were characterized by IR, ^{1}H NMR, elemental analyses, and single-crystal X-ray diffraction analyses. The two

(13) *SAINT+*, version 6.2a. Bruker Analytical X-ray System, Inc.: Madison, Wisconsin, U.S.A., 2001.
(14) Sheldrick, G. M. *SHELXTL*, version 6.1; Bruker Analytical X-ray Systems, Inc.: Madison, Wisconsin, U.S.A., 1997.
(15) (a) Hall, M. B.; Fenske, R. F. *Inorg. Chem.* **1972**, *11*, 768−775. (b) Webster, C. E.; Hall, M. B. In *Theory and Applications of Computational Chemistry: The First Forty Years*; Dykstra, C., Ed.; Elsevier: Amsterdam, 2005; Chapter 40, pp 1143−1165.
(16) Manson, J.; Webster, C. E.; Hall, M. B. *JIMP*, development version 0.1.v117 (built for Windows PC and Redhat Linux); Department of Chemistry, Texas A&M University: College Station, TX; http:// www.chem.tamu.edu/jimp/, accessed July 2004.
(17) Lichtenberger, D. L. *MOPLOT2 for orbital and density plots from linear combinations of Slater or Gaussian type orbitals*, version 2.0; Department of Chemistry, University of Arizona: Tucson, AZ, 1993.

Table 2. Crystallographic Data for Compounds **14**, **15**, and **16**

compound	**14**	**15**	**16**
empirical formula	$PtRuSnPO_4C_{42}H_{49}\cdot{}^3/_2C_6H_6$	$PtRuSnPO_4C_{42}H_{49}$	$PdRuSnPO_4C_{42}H_{49}$
formula weight	1180.79	1063.63	974.94
crystal system	triclinic	triclinic	triclinic
lattice parameters			
a (Å)	12.9837(3)	10.3182(2)	11.5256(5)
b (Å)	13.3071(3)	12.2019(3)	12.7825(6)
c (Å)	14.9483(4)	18.4334(4)	17.0037(8)
α (deg)	98.206(1)	78.227(1)	101.212(1)
β (deg)	90.739(1)	78.186(1)	106.474(1)
γ (deg)	104.088(1)	66.084(1)	103.063(1)
V (Å^3)	2476.31(10)	2057.51(8)	2248.67(18)
space group	$P\bar{1}$ (#2)	$P\bar{1}$ (#2)	$P\bar{1}$ (#2)
Z value	2	2	2
ρ_{calcd} (g/cm^3)	1.584	1.717	1.440
μ (Mo Kα) (mm^{-1})	3.692	4.433	1.349
temperature (K)	294(2)	294(2)	294(2)
$2\Theta_{max}$ (deg)	56.6	56.6	56.6
no. obsd ($I > 2\sigma(I)$)	9883	8334	8009
no. parameters	503	468	468
goodness of fit GOF[a]	1.039	1.024	1.042
max. shift in cycle	0.001	0.002	0.001
residuals:[a] R1, wR2	0.0339, 0.0773	0.0322, 0.0638	0.0469, 0.1532
absorption correction, max/min	multi-scan 1.000/0.754	multi-scan 1.000/0.828	multi-scan 1.000/0.580
largest peak in final diff map (e$^-$/Å^3)	1.174	1.136	1.707

[a] $R = \Sigma_{hkl}(||F_{obsd}| - |F_{calcd}||)/\Sigma_{hkl}|F_{obsd}|$; $R_w = [\Sigma_{hkl}w(|F_{obsd}| - |F_{calcd}|)^2/\Sigma_{hkl}wF_{obsd}^2]^{1/2}$, $w = 1/\sigma^2(F_{obsd})$; GOF $= [\Sigma_{hkl}w(|F_{obsd}| - |F_{calcd}|)^2/(n_{data} - n_{vari})]^{1/2}$.

Table 3. Crystallographic Data for Compounds **17** and **18**

compound	**17**	**18**
empirical formula	$PtOsPO_4C_{34}H_{43}$	$PtOsSnPO_3C_{49}H_{55}$
formula weight	1050.63	1226.88
crystal system	monoclinic	triclinic
lattice parameters		
a (Å)	15.3785(8)	9.9318(3)
b (Å)	12.0732(6)	12.0190(3)
c (Å)	20.6568(10)	19.9237(5)
α (deg)	90	94.884(1)
β (deg)	108.841(1)	91.471(1)
γ (deg)	90	106.541(1)
V (Å^3)	3629.8(3)	2268.49(11)
space group	$P2_1/n$ (#14)	$P\bar{1}$ (#2)
Z value	4	2
ρ_{calcd} (g/cm^3)	1.923	1.796
μ (Mo Kα) (mm^{-1})	8.096	6.490
temperature (K)	294(2)	294(2)
$2\Theta_{max}$ (deg)	56.7	56.6
no. obsd ($I > 2\sigma(I)$)	6971	8777
no. parameters	391	526
goodness of fit GOF[a]	1.031	1.065
max shift in cycle	0.002	0.005
residuals:[a] R1, wR2	0.0376, 0.0961	0.0381, 0.0753
absorption correction, max/min	multi-scan 1.000/0.757	multi-scan 1.000/0.430
largest peak in final diff map (e$^-$/Å^3)	3.068	1.436

[a] $R = \Sigma_{hkl}(||F_{obsd}| - |F_{calcd}||)/\Sigma_{hkl}|F_{obsd}|$; $R_w = [\Sigma_{hkl}w(|F_{obsd}| - |F_{calcd}|)^2/\Sigma_{hkl}wF_{obsd}^2]^{1/2}$, $w = 1/\sigma^2(F_{obsd})$; GOF $= [\Sigma_{hkl}w(|F_{obsd}| - |F_{calcd}|)^2/(n_{data} - n_{vari})]^{1/2}$.

products are isomers formed by the addition of 1 equiv of PhC_2H and 1 equiv of Pt(PBu$^t_3$) to **10**. There are two crystallographically independent molecules in the asymmetric crystal unit of **12**. Both molecules are structurally similar. An ORTEP diagram of the molecular structure of one of the two independent molecules of **12** is shown in Figure 1. The platinum atom is bonded to the osmium atom at a normal bonding distance, Pt(1)−Os(1) = 2.7198(4) Å (molecule 1) and [Pt(2)−Os(2) = 2.7177(4) Å] (molecule 2). There is an η^2-bridging HCC(H)Ph ligand that is σ-bonded to the platinum atom, Pt(1)−C(1) = 2.012(6) Å [Pt(2)−C(3) = 2.017(6) Å] and π-bonded to the osmium atom: Os(1)−C(1) = 2.246(7) Å, Os(1)−C(2) = 2.364(6) Å and [Os(2)−C(3) = 2.243(7) Å, Os(2)−C(4) = 2.375(6) Å] (molecule 2). The C−C bond distance for the alkenyl ligand is C(1)−C(2) = 1.409(10) Å and [C(3)−C(4) = 1.392(9) Å]. This is similar to the C−C bond distance of 1.38(4) Å found for the alkenyl ligand in the compound $HOs_3(CO)_{10}$(HCC(H)Bu^t)[18a] and for alkenyl ligands in related complexes.[18b] The $SnPh_3$ ligand on the osmium atom is positioned *trans* to the Pt

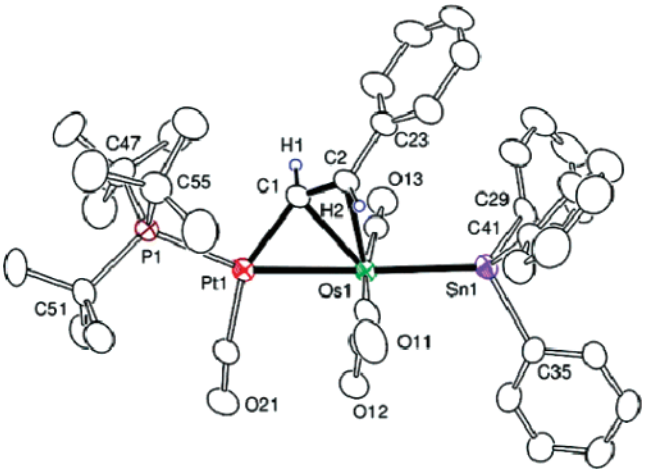

Figure 1. An ORTEP diagram of the molecular structure of **12** showing 30% probability thermal ellipsoids. Selected bond distances (in Å) are as follows: (molecule 1) Pt(1)−Os(1) = 2.7198(4), Pt(1)−C(1) = 2.012(6), Os(1)−C(1) = 2.246(7), Os(1)−C(2) = 2.364(6), Pt(1)−P(1) = 2.3446(17), Os(1)−Sn(1) = 2.6921(5); (molecule 2) Pt(2)−Os(2) = 2.7177(4), Pt(2)−C(3) = 2.017(6), Os(2)−C(3) = 2.243(7), Os(2)−C(4) = 2.375(6), Pt(2)−P(2) = 2.3432(17), Os(2)−Sn(2) = 2.6840(5), C(1)−C(2) = 1.409(10), C(3)−C(4) = 1.392(9), Sn(1)−Os(1) − Pt(1) = 165.184(17), Sn(2)−Os(2)−Pt(2) = 163.966(15).

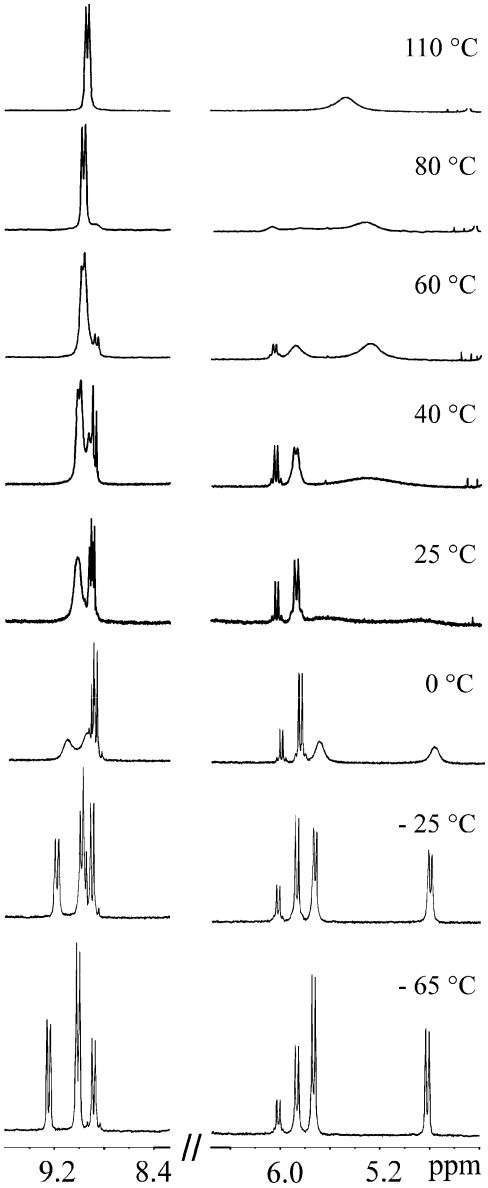

Figure 2. Variable temperature ^{1}H NMR spectra for compound **12** in toluene-d_8 solvent. Resonance of the phenyl protons (6.6−8.3 ppm) have been removed for clarity.

atom, Sn(1)−Os(1)−Pt(1) = 165.184(17)° [Sn(2)−Os(2)−Pt(2) = 163.966(15)°]. The Os−Sn distance, Os(1)−Sn(1) = 2.6921(5) Å [Os(2)−Sn(2) = 2.6840(5) Å] is slightly shorter than that found in **10**, 2.7382(2) Å.[11]

The ^{1}H NMR spectra of **12** at −65 °C indicates that it exists in solution as a mixture of four isomers. At room temperature the isomers are interconverting rapidly on the ^{1}H NMR time scale. A stacked plot of the variable temperature ^{1}H NMR spectra of the two alkenyl protons of **12** in the region 4.8−9.5 ppm is shown in Figure 2. The region of the resonances of the phenyl protons (6.6−8.3 ppm) has been removed for clarity. At −65 °C, there are four doublets of varying intensities in the region 4.8−6.2 ppm. These resonances are assigned to the alkenyl proton H(1), cf. Figure 1. One doublet corresponds to each of four isomers in solution. At −65 °C, there are another

Scheme 3

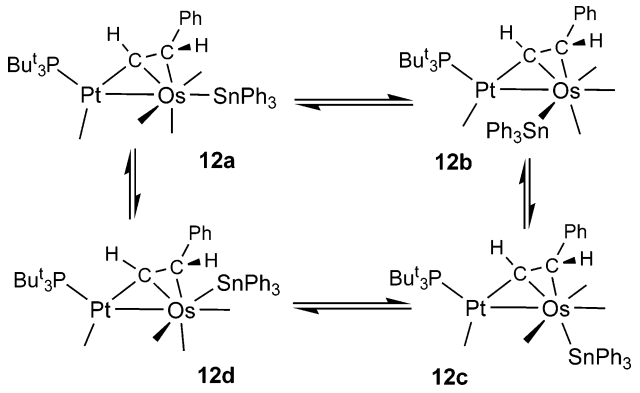

three doublets of varying intensities in the region 8.5−9.5 ppm. These can be assigned to the proton H(2) of the four isomers of **12**, cf. Figure 1. Although there should be four doublets for the four isomers, this can be explained by an accidental shift equivalence of two sets of doublets at 9.01 ppm. This is confirmed by the spectrum recorded at −25 °C where the resonance at 9.01 has been split into two overlapping doublets as a result of different temperature dependent changes in the chemical shifts of the two doublets that were superimposed at 9.01 ppm at −65 °C. Over the temperature range −65 °C to +110 °C three dynamical averaging processes are observed. At 0 °C two pairs of doublets in the 4.8−6.2 ppm and 8.5−9.5 ppm regions of the spectrum exhibit broadening due to dynamical exchange. These pairs of resonances have averaged in their respective regions at +60 °C. At about 40 °C, another pair of doublets, one in the 4.8−6.2 ppm region and one in the 8.5−9.5 ppm region from a third isomer, begins to broaden and ultimately averages with the resonances of the other averaging isomers at higher temperatures. Finally, at about 60 °C, the fourth pair of doublets begins to broaden (this is clear at +80 °C) and then averages with the average of the resonances of the other three isomers. The temperature dependent changes are fully reversible. At +110 °C, the resonances in each of the two regions have averaged completely. The averaged doublet at 9.1 ppm is sharp, but due to the greater chemical shift differences between the resonances, the averaged resonance at about 5.4 ppm has not fully sharpened yet at 110 °C which is the highest temperature at which we could record in the toluene-d_8 solvent that was used for this sample. It is proposed that the four isomers of **12**, **12a**−**12d**, consist of the one found in the solid state shown in Figure 1 and three others formed by interchanging the $SnPh_3$ group with each of the three terminal CO ligands on the osmium atom. Specific assignments cannot be made. These four isomers can be interchanged at three different rates (as observed) simply by performing internal rotations of the entire Pt(1)−C(1)−C(2) group to four different rotational orientations each ∼90° apart with respect to the Os(CO)$_3$(SnPh$_3$) group; see Scheme 3. Slight angle deformations occur between the $SnPh_3$ and CO ligands during these rotations, but this would not introduce any significant barriers. The Pt(1)−C(1)−C(2) group could be viewed as a π-bonded metallaallyl fragment. Internal rotations of π-allyl ligands are well documented.[19] The resonances of the *tert*-butyl methyl resonances (not shown in Figure 2) are complex throughout the low-

(18) (a) Sappa, E.; Tiripicchio, A.; Lanfredi, A. M. M. *J. Organomet. Chem.* **1975**, *249*, 391−404. (b) Deeming, A. J. *Adv. Organomet. Chem.* **1986**, *26*, 1−96.

(19) Davison, A.; Rode, W. C. *Inorg. Chem.* **1967**, *6*, 2124−2125.

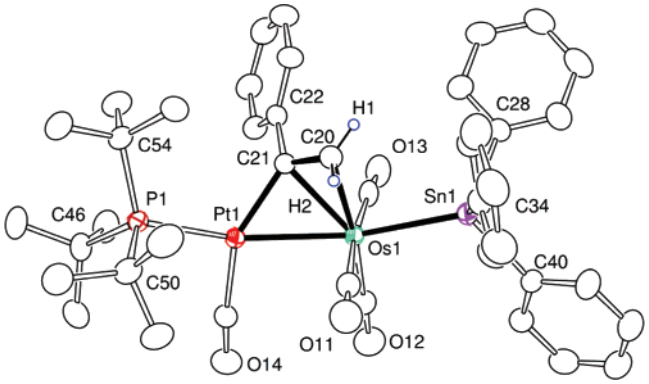

Figure 3. ORTEP diagram of the molecular structure of **13** showing 40% probability thermal ellipsoids. Selected bond distances (Å) and angles (deg) are as follows: Pt(1)−Os(1) = 2.7114(2), Pt(1)−P(1) = 2.3575(9), Pt(1)−C(21) = 2.023(4), Os(1)−C(21) = 2.300(4), Os(1)−C(20)= 2.300(4), Os(1)−Sn(1) = 2.6743(3), C(20)−C(21) = 1.403(6); Sn(1)−Os(1)−Pt(1) = 153.704(9).

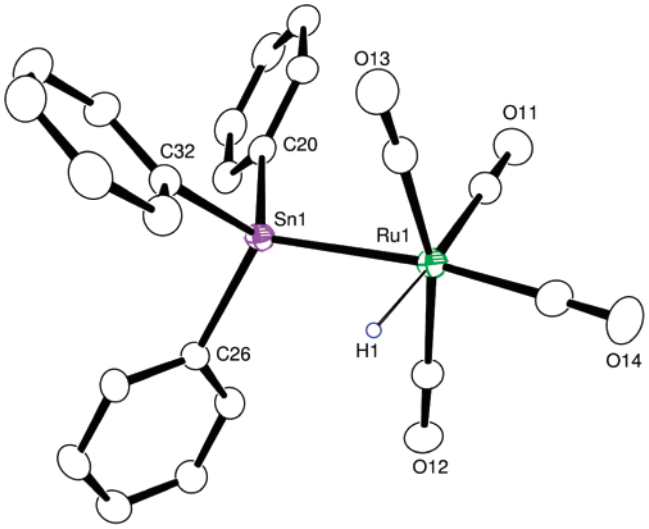

Figure 4. An ORTEP diagram of the molecular structure of **11** showing 30% probability thermal ellipsoids. Selected bond distances (in Å) are as follows: Ru(1)−Sn(1) = 2.7108(3), Ru(1)−H(1) = 1.63(4), Sn(1)−C(20) = 2.148(3), Sn(1)−C(26) = 2.157(3), Sn(1)−C(32) = 2.156(3).

temperature range due to hindered internal rotations of the *tert*-butyl groups about the P−C bonds, but at +60 °C a single doublet is observed, as expected for the average of the four isomers.

The $HC_2(H)Ph$ ligand in **12** was formed by the insertion of the PhC_2H molecule into the Os−H bond with transfer of the hydrogen atom to the phenyl-substituted carbon atom of the alkyne. Note the *E*-stereochemistry of the alkenyl ligand which is consistent with cis insertion of the alkyne via the classical four-center transition state.[9] In the course of the PhC_2H addition, one CO ligand from **10** was shifted from the osmium atom to the platinum atom. The osmium atom in **12** contains 18 valence electrons; the platinum atom has only 16.

An ORTEP diagram of the molecular structure of **13** is shown in Figure 3. The structure of **13** is very similar to that of **12**. There is a platinum−osmium bond that is only slightly shorter than that in **12**, Pt(1)−Os(1) = 2.7114(4) Å. There is also an η^2-bridging alkenyl ligand, this time with the formula $PhCCH_2$, that is σ-bonded to the platinum atom, Pt(1)−C(21) = 2.023(4) Å, and π-bonded to the osmium atom, Os(1)−C(21) = 2.300(4) Å, Os(1)−C(20) = 2.300(4) Å. The C−C bond distance, C(20)−C(21) = 1.403(6) Å, is similar to that in **12**. The $SnPh_3$ ligand on the Os atom is also positioned *trans* to the Pt atom, Sn(1)−Os(1)−Pt(1) = 153.704(9)°. The Os−Sn distance in **13**, Os(1)−Sn(1) = 2.6743(3) Å, is similar to that found in **12**. The ^{1}H NMR spectra of **13** are consistent with the structure found in the solid state indicating the presence of only one isomer in solution. The small two bond coupling, $^2J_{H-H}$ = 1.6 Hz, between the two resonances at δ = 4.82 and 2.81 is consistent with the presence of the two hydrogen atoms on the same carbon atom C(20) of the $PhCCH_2$ ligand. The $PhCCH_2$ ligand could be formed by insertion of the PhC_2H molecule into the Os−H bond by a mechanism analogous to that which yielded **12**, except that the hydrogen atom would be transferred instead to the unsubstituted carbon atom of the alkyne; see below for further discussion of the mechanism.

For comparative purposes, the reactions of $HRu(CO)_4SnPh_3$, **11**, with PhC_2H in the presence and absence of Pt(PBu$^t_3$)$_2$ were also investigated. The new compound **11** was obtained in 49% yield from the reaction of $Ru(CO)_5$ with $HSnPh_3$ by heating a solution in hexane solvent to reflux for 10 min. Compound **11** was characterized by IR, ^{1}H NMR, and single-crystal X-ray diffraction analysis. An ORTEP diagram of the molecular structure of **11** is shown in Figure 4. Compound **11** is structurally similar to **10**. The ruthenium atom contains four terminal carbonyl ligands. The $SnPh_3$ ligand and terminal hydrido ligand occupy *cis*-coordination sites in the six-coordinate complex. The Ru−H distance, 1.63(4) Å, is similar to the Os−H distance in **10**, 1.67(4) Å.[11] The hydrido ligand exhibits the expected high field proton resonance shift in the ^{1}H NMR spectrum δ = −7.66 with coupling to the tin atom, $^2J_{119_{Sn-H}}$ = 51 Hz, $^2J_{117_{Sn-H}}$ = 49 Hz.

Like **10**, compound **11** does not react with PhC_2H at temperatures less than 68 °C, where it begins to decompose. However, in the presence of Pt(PBu$^t_3$)$_2$, there is a rapid reaction at room temperature to yield two new compounds: $PtRu(CO)_4(SnPh_3)(PBu^t_3)[\mu$-HCC(H)Ph], **14**, and $PtRu(CO)_4(SnPh_3)(PBu^t_3)[\mu$-$H_2CCPh]$, **15**, in the yields 33% and 5%, respectively. Compounds **14** and **15** have been shown to be the Ru homologues of **12** and **13** by a combination of IR, ^{1}H NMR, and single-crystal X-ray diffraction analyses. ORTEP diagrams of the molecular structures of **14** and **15** are shown in Figures 5 and 6, respectively.

The molecular structure of **14** is similar to that of **12**, except that the $SnPh_3$ ligand on the Ru atom is positioned *cis* to the Pt atom, Sn(1)−Ru(1)−Pt(1) = 101.098(12)°. This structure would correspond to the solution isomer **12c** proposed for **12**. The Ru−Sn bond distance, Ru(1)−Sn(1) = 2.6585(4) Å, is significantly shorter than that in **11**, 2.7108(3) Å. The Pt−Ru bond distance, Pt(1)−Ru(1) = 2.6981(3) Å, is only slightly shorter than the Pt−Os bond distance in **12**. Compound **14** was formed by the insertion of the PhC_2H molecule into the Os−H bond with transfer of the hydrido ligand to the phenyl-substituted carbon atom. The Pt−C and Ru−C distances to the bridging $HC_2(H)$-Ph ligand are very similar to those found in **12**: Pt(1)−C(1) = 2.022(4) Å, Ru(1)−C(1) = 2.239(4) Å, and Ru(1)−C(2) = 2.377(4) Å. Like **12**, compound **14** also exists in solution, as a mixture of interconverting isomers. This was demonstrated by the variable temperature ^{1}H NMR spectra that are shown in Figure 7. These spectral changes can be explained by the presence of isomers with dynamical interconversions similar

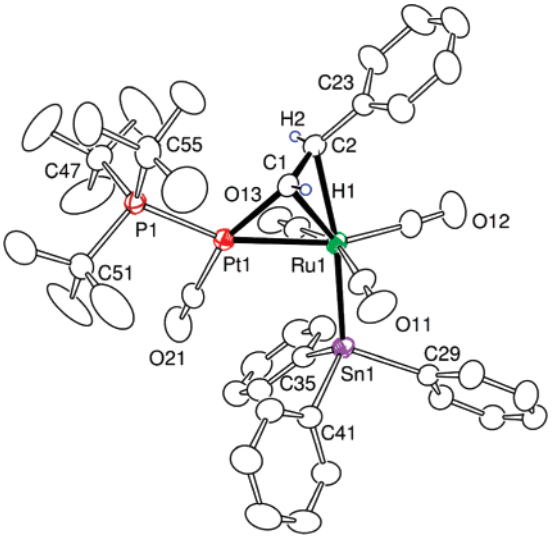

Figure 5. ORTEP diagram of the molecular structure of **14** showing 30% probability thermal ellipsoids. Selected bond distances (in Å) and angles (deg) are as follows: Pt(1)−Ru(1) = 2.6981(3), Pt(1)−P(1) = 2.3542(10), Pt(1)−C(1) = 2.022(4), Ru(1)−C(1) = 2.239(4), Ru(1)−C(2) = 2.377(4), Ru(1)−Sn(1) = 2.6585(4), C(1)−H(1) = 1.04(4), C(2)−H(2) = 0.90(4); Sn(1)−Ru(1)−Pt(1) = 101.098(12).

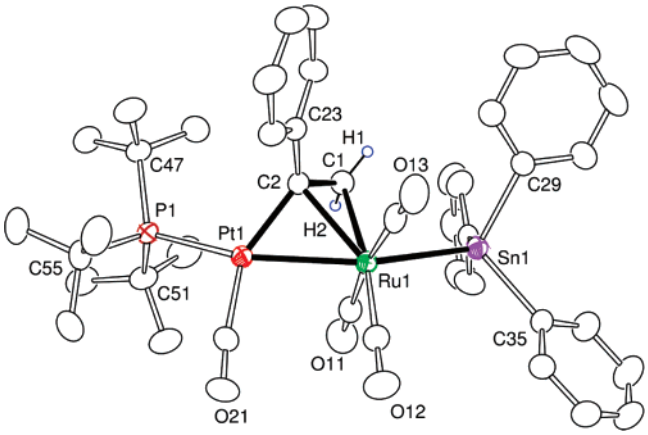

Figure 6. ORTEP diagram of the molecular structure of **15** showing 30% probability thermal ellipsoids. Selected bond distances (in Å) and angles (deg) are as follows: Pt(1)−Ru(1) = 2.7068(4), Pt(1)−P(1) = 2.3573(10), Pt(1)−C(2) = 2.023(4), Ru(1)−C(1) = 2.292(4), Ru(1)−C(2) = 2.298(4), Ru(1)−Sn(1) = 2.6612(4), C(1)−H(1) = 0.90(4), C(1)−H(2) = 1.10(4); Sn(1)−Ru(1)−Pt(1) = 153.786(16).

to those shown for **12** in Scheme 1, but their relative amounts are different from those found for **12**. Specific assignments cannot be made at this time.

Compound **15** is an isomer of **14**. It is structurally similar to **13**. The Pt−Ru and Ru−Sn bond distances are similar to those in **14**, Pt(1)−Ru(1) = 2.7068(4) Å, Ru(1)−Sn(1) = 2.6612(4) Å. The $SnPh_3$ ligand lies approximately *trans* to the Pt atom, Sn(1)−Ru(1)−Pt(1) = 153.786(16)°. Compound **15** was formed by the insertion of the PhC_2H molecule into the Ru−H bond with transfer of the hydrido ligand to the unsubstituted carbon atom. Both hydrogen atoms on the alkenyl carbon atom C(1) were located and refined in the structural analysis. They were also confirmed at C(1) by ^{1}H NMR spectroscopy by the observation of their resonances at δ = 4.51 and 2.80 ppm. The resonance at 4.51 ppm appears as a broad singlet due to small couplings to ^{31}P from the phosphine ligand and the other hydrogen atom on C(1), $^4J_{P-H}$ = 2.9 Hz and $^2J_{H-H}$ = 1.4 Hz.

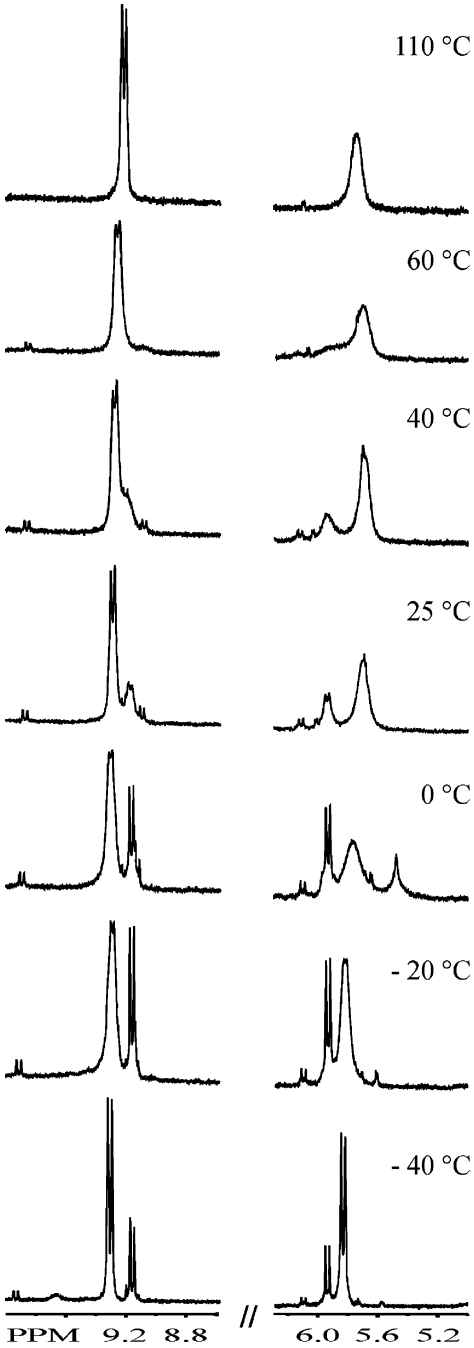

Figure 7. Variable temperature ^{1}H NMR spectra for compound **14** in toluene-d_8 solvent. Resonance of the phenyl protons (6.4−8.2 ppm) have been removed for clarity.

The reaction of **11** with PhC_2H in the presence of $Pd(PBu^t_3)_2$ was also investigated. Only one alkyne addition product was obtained, $PdRu(CO)_4(SnPh_3)(PBu^t_3)[\mu$-$H_2CCPh]$, **16** (15% yield), when a solution of **11** with PhC_2H and $Pd(PBu^t_3)_2$ in methylene chloride solvent was heated to reflux for 10 min. Compound **16** was characterized by a combination of IR, ^{1}H NMR, and single-crystal X-ray diffraction analyses. An ORTEP diagram of the molecular structure of **16** is shown in Figure 8. Compound **16** was formed by the addition and insertion of 1 equiv of PhC_2H into the Ru−H bond of **12** with transfer of the hydrogen atom to the unsubstituted carbon atom of the alkyne. $Pd(PBu^t_3)$ (1 equiv) was also added to the complex, but unlike the H_2C_2Ph ligands in **13** and **15**, the bridging H_2C_2Ph ligand in **16** is

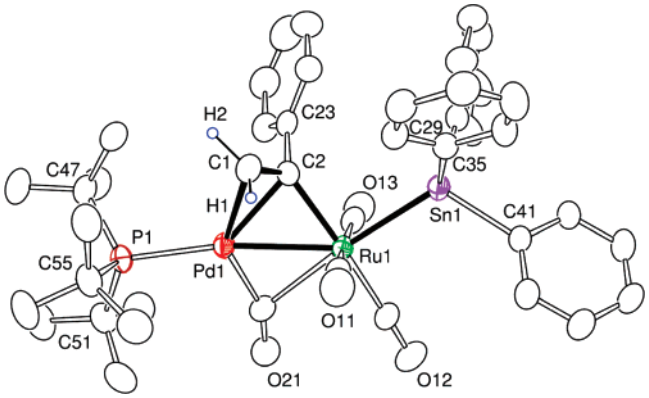

Figure 8. ORTEP diagram of the molecular structure of **16** showing 30% probability thermal ellipsoids. Selected bond distances (in Å) and angles (deg) are as follows: Pd(1)−Ru(1) = 2.7122(5), Pd(1)−P(1) = 2.3681(13), Pd(1)−C(2) = 2.250(5), Pd(1)−C(1) = 2.357(6), Ru(1)−C(2) = 2.152(5), Ru(1)−Sn(1) = 2.6587(5), C(1)−H(1) = 0.89(4), C(1)−H(2) = 1.13(7); Sn(1)−Ru(1)−Pd(1) = 143.462(19), C(21)−Ru(1)−Sn(1) = 173.33(13).

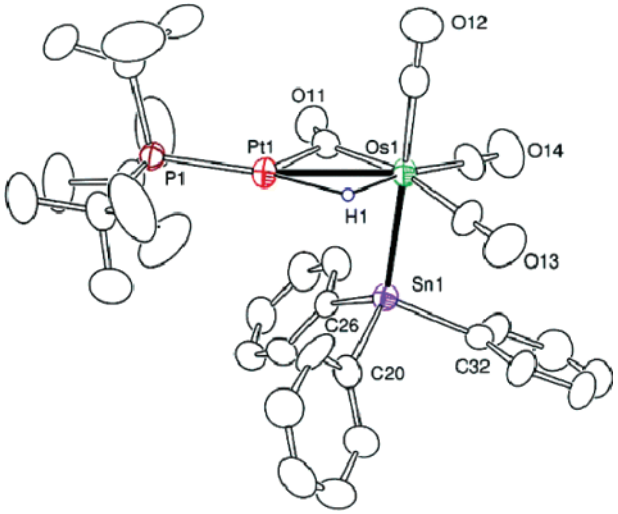

Figure 9. ORTEP diagram of the molecular structure of **17** showing 40% probability thermal ellipsoids. Selected bond distances (in Å) angles (deg) are as follows: Pt(1)−Os(1) = 2.7628(3), Pt(1)−P(1) = 2.2808(14), Pt(1)−C(11) = 1.982(6), Pt(1)−H(1) = 1.92(6), Os(1)−C(11) = 2.071(6), Os(1)−Sn(1) = 2.7281(5), Os(1)−H(1) = 1.95(6); Sn(1)−Os(1)−Pt(1) = 84.652(12).

σ-bonded to the ruthenium atom and π-bonded to the palladium atom. This changes its electron donation properties, and as a result, the CO ligand that was terminal on the Pt atom in compounds **12**−**15** occupies instead a position bridging the two metal atoms in **16**. The $SnPh_3$ ligand on **16** is nearly trans to the carbon atom C(21) of the bridging CO ligand, C(21)−Ru(1)−Sn(1) = 173.33(13)° instead of being trans to the Pd atom, Sn(1)−Ru(1)−Pd(1) = 143.462(19)°. The Pd−Ru distance is typical of Pd−Ru single bonds, Pd(1)−Ru(1) = 2.7122(5) Å. In fact, this is significantly shorter than the Ru−Pd distances found in **1**, 2.7877(12)−2.8398(11) Å.[1a] In the presence of a Pd−Ru single bond, the Pd has a 16 electron configuration and the Ru atom has 18 electrons. Its ^{1}H NMR spectrum indicates that **16** exists only as one isomer in solution. Both hydrogen atoms on the alkenyl carbon atom C(1) were located and refined in the structural analysis. They were also confirmed by ^{1}H NMR spectroscopy by the observation of their resonances at δ = 5.53 and 4.42 ppm. The small coupling $^2J_{H-H}$ = 2 Hz between them is consistent with their *gem*-position.

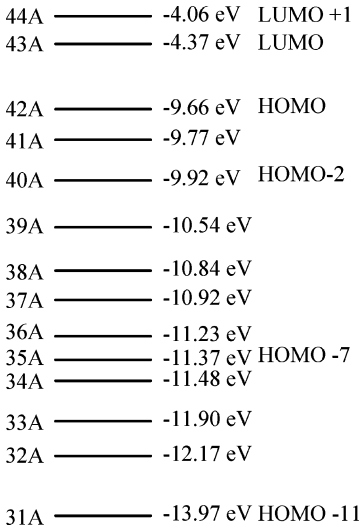

Figure 10. Energy level diagram of the Fenske−Hall molecular orbitals of **17** with the corresponding orbital energies listed in electron volts (eV).

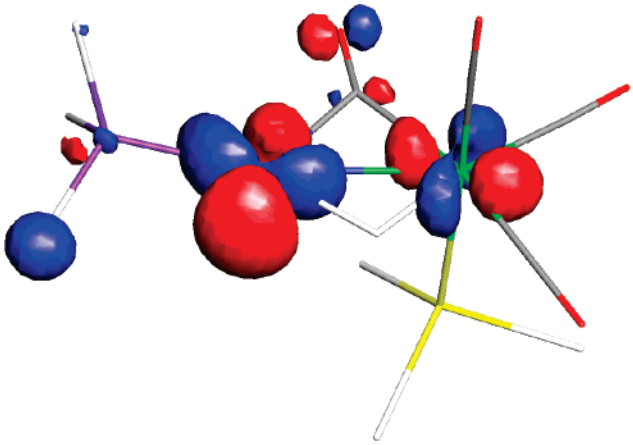

Figure 11. A contour diagram of the Fenske−Hall LUMO, 43A of **17**.

To try to learn more about how the M(PBu$^t_3$), M = Pt, Pd, groups have activated **10** and **11** toward this PhC_2H insertion reaction, we have investigated the reaction of **10** with Pt(PBu$^t_3$)$_2$ in the absence of PhC_2H. When Pt(PBu$^t_3$)$_2$ was added to a solution of **10** in CH_2Cl_2 at room temperature for 25 min, the new compound $PtOs(CO)_4(SnPh_3)(PBu^t_3)(\mu$-H), **17**, was formed and subsequently isolated in 45% yield by TLC on silica gel. Compound **17** was also characterized by a combination of IR, ^{1}H NMR, and single-crystal X-ray diffraction analyses.

An ORTEP diagram of the molecular structure of **17** is shown in Figure 9. The molecule can be viewed most simply as a Pt(PBu$^t_3$) adduct of **10**. The 12 electron Pt(PBu$^t_3$) fragment has formed bonding interactions with the osmium atom, the hydrido ligand, and one of the CO ligands of **10**. The Pt−Os distance, Pt(1)−Os(1) = 2.7628(3) Å, is significantly longer than that in **12** and **13**. The shortness of the Pt−Os bonds in **12** and **13** can be attributed to the presence of the bridging alkenyl ligands, while the bridging hydrido ligand in **17** may produce a lengthening effect on the Pt−Os bond in that complex.[20] The $SnPh_3$ ligand on the Os atom is also positioned *cis* to the Pt atom, Sn(1)−Os(1)−Pt(1) = 84.652(12)°. The Os−Sn distance, Os(1)−Sn(1) = 2.7281(5) Å, is slightly longer than those found in **12** and **13**. The hydrido ligand was located and refined

(20) Teller, R. G.; Bau, R. *Struct. Bonding* **1981**, *44*, 1−82.

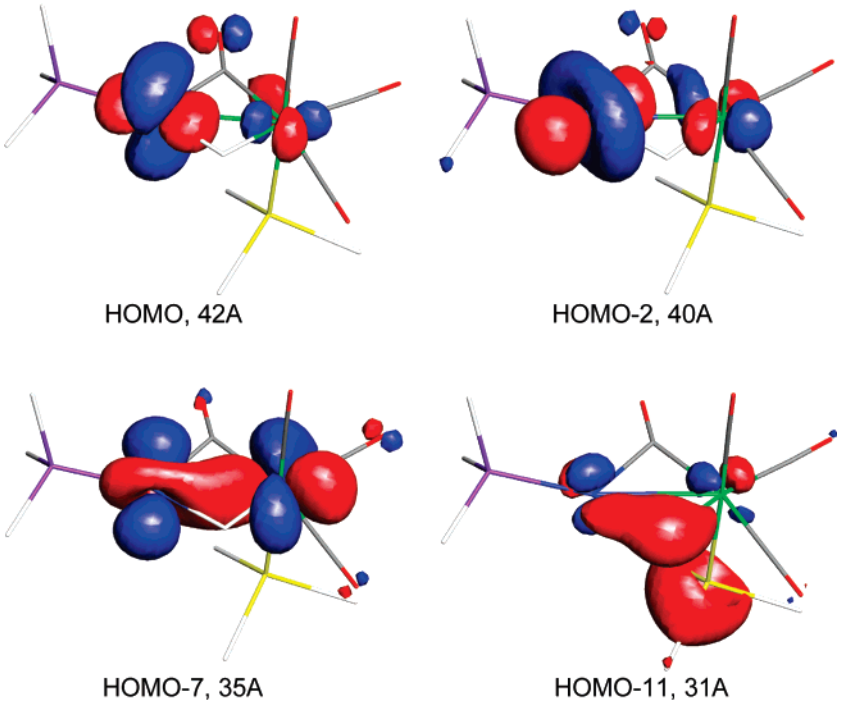

Figure 12. Molecular orbitals responsible for the bonding interactions in **17** (**31A**, **35A**, **40A**, **42A**).

Scheme 4

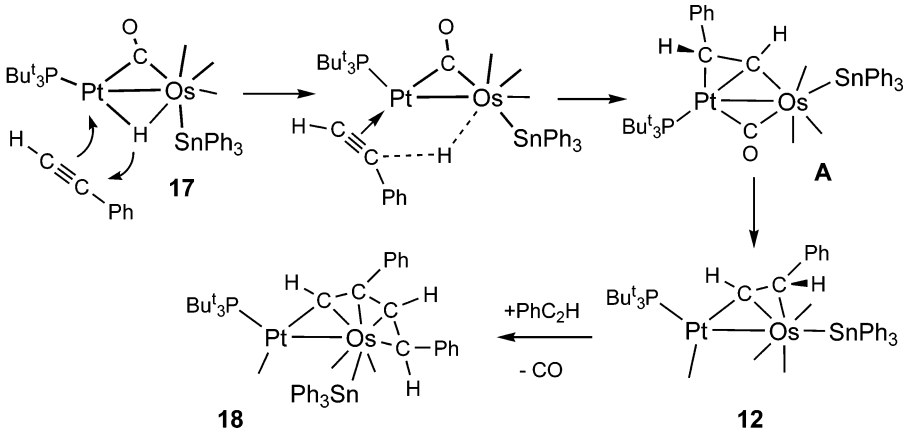

crystallographically, Pt(1)−H(1) = 1.92(6) Å and Os(1)−H(1) = 1.95(6) Å, and confirmed by its high field ^{1}H NMR chemical shift, $\delta = -5.99$ with its couplings to P, Pt, and Sn, $^2J_{P-H} =$ 46 Hz, $^1J_{Pt-H} = 566$ Hz, $^2J_{119Sn-H} = 46$ Hz, $^2J_{117Sn-H} = 44$ Hz. The Os−H bond distance is much longer than that in **10**, 1.67(4) Å.[11] Most importantly, when **17** was treated with PhC_2H, it was converted to **12** in 28% yield. No additional quantities of $Pt(PBu^t_3)_2$ are needed to promote the reaction. Thus, we feel that **17** is most likely an intermediate in the formation of **12**.

To understand the electronic structure in **17** and its possible role in the reaction of **17** with PhC_2H, Fenske−Hall molecular orbitals of **17** were calculated.[15] For this calculation, the atomic coordinates from the crystal structure were used, and the *tert*-butyl groups on the PBu^t_3 ligand and the phenyl groups on the $SnPh_3$ ligand were replaced with hydrogen, e.g., PH_3 and SnH_3. An energy level diagram showing the frontier orbitals is shown in Figure 10. The LUMO 43A (see Figure 11) and the HOMO 42A, HOMO−2 40A, HOMO−7 35A, and HOMO−11 31A (see Figure 12) are key orbitals. Diagrams of the complete set of molecular orbitals LUMO+2 to HOMO−13 are available, see Supporting Information. There is a significant energy gap, 5.29 eV, between the HOMO and LUMO. The LUMO is largely the antibonding equivalent of an interaction of the two metal atoms with the π-bond of the bridging CO ligand, C(11)−O(11). The bonding counterpart of this orbital is represented by the HOMO−2, in which the d-orbital on the Pt atom has a slightly different hybridization than that in the LUMO. The HOMO 42A is largely "nonbonding" in character and is composed of atomic d-orbitals localized largely on the two metal atoms. The Pt−Os bond is shown clearly in Figure 12 in the HOMO−7 orbital. Another important orbital is shown by the HOMO−11 31A which shows the bond between the hydrido ligand and the two metal atoms. This orbital is important because it shows how the Pt atom activates the Os−H bond. The molecular orbitals show clearly the types of interactions that we would expect for **10**, but more importantly the LUMO reveals a feature of the electronic structure that may provide additional insight into the nature of the addition and insertion of the alkyne into the Os−H bond. In particular, the LUMO contains a large com-

ponent on the platinum atom. We believe that this empty orbital serves as the landing site for the alkyne in its initial interactions with **17**.

Proposed Mechanism of Os−H Activation and Alkyne Insertion. The reaction of **10** with PhC_2H in the presence of Pt(PBu$^t_3$)$_2$ begins with the formation of **17** by loss of one PBu$^t_3$ ligand from Pt(PBu$^t_3$)$_2$. The empty orbital that is formed on the Pt(PBu$^t_3$) fragment then forms a bonding interaction with the Os−H bond and one of the CO ligands of **10**. The Os−H bond is weakened with the formation of **17**. The rest of the process is shown in Scheme 4. The alkyne PhC_2H then adds to the LUMO of **17** at the platinum atom. Insertion of the alkyne ligand into the Pt−H bond of the bridging hydrido ligand initiates C−H bond formation. This may involve a four atom transition state.[9] The hydrido ligand could be shifted to either of the alkyne carbon atoms. This will produce an alkenyl ligand either HC_2-(H)Ph or PhC_2H_2 that subsequently adopts a conventional η^2-σ-π-bridging coordination mode. If the alkyne does indeed interact with the platinum atom in the initial contact with **17**, then the bridging alkenyl ligand may initially adopt a bridging mode with its π-bonding to the platinum atom, species **A** in Scheme 4. The viability of the intermediate **A** is supported by the observed structure of **16**. For the osmium−platinum compounds, a rearrangement follows the formation of **A** in which the alkenyl ligand shifts its π-coordination to the osmium atom and the bridging CO ligand then shifts to a terminal site on the platinum atom to yield either **12** or **13** depending upon which carbon atom of the acetylene received the hydrido ligand. Shapley showed that bridging alkenyl ligands could readily alternate their π-bonding between adjacent metal atoms.[21]

Similar mechanisms can explain the formation of **14** and **15** from the reactions of **11** with phenylacetylene and Pt(PBu$^t_3$)$_2$.

The platinum atoms in each of the compounds **12**−**15** and **17** and the palladium atom in **16** have 16 electron configurations and could add yet another equivalent of PhC_2H under the appropriate conditions. In fact, we have found that such an addition does occur to **12** under mild conditions.

When a solution of **12** and PhC_2H in CH_2Cl_2 solvent was heated to reflux for 60 min, the new compound $PtOs(CO)_3$-$(SnPh_3)$(PBu$^t_3$)[μ-HCC(Ph)C(H)C(H)Ph], **18**, was obtained in 48% yield. Compound **18** was characterized by IR, ^{1}H NMR, and single-crystal X-ray diffraction analyses. An ORTEP diagram of **18** is shown in Figure 13. Compound **18** contains a bridging 2,4-diphenylbutadienyl ligand, HCC(Ph)C(H)C(H)Ph. The four carbon atoms C(20), C(21), C(22), and C(23) are π-bonded to the osmium atom, Os(1)−C(20) = 2.253(6) Å, Os-(1)−C(21) = 2.292(6) Å, Os(1)−C(22) = 2.230(6) Å, Os(1)−C(23) = 2.369(6) Å. C(20) is also σ-bonded to the platinum atom, Pt(1)−C(20) = 2.017(6) Å. The bonds C(20)−C(21) = 1.416(8) Å and C(22)−C(23) = 1.396(8) Å are significantly

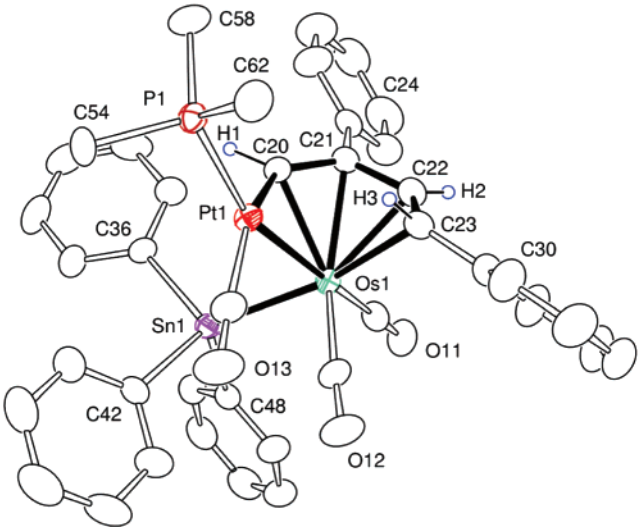

Figure 13. An ORTEP diagram of the molecular structure of **18** showing 30% probability thermal ellipsoids. The methyl groups are not shown for clarity. Selected bond distances (in Å) and angles (deg) are as follows: Pt(1)−P(1) = 2.3601(15), Pt(1)−Os(1) = 2.7255(3), Pt(1)−C(20) = 2.017-(6), Os(1)−C(20) = 2.253(6), Os(1)−C(21) = 2.292(6), Os(1)−C(22) = 2.230(6), Os(1)−C(23) = 2.369(6), Os(1)−Sn(1) = 2.6540(4), C(20)−C(21) = 1.416(8), C(21)−C(22) = 1.446(8), C(22)−C(23) = 1.396(8); Sn(1)−Os(1)−Pt(1) = 90.456(12).

shorter than C(21)−C(22) = 1.446(8) Å and indicate that the diene character of this ligand is still present when it is coordinated. There is a Pt−Os bond, Pt(1)−Os(1) = 2.7255(3) Å, which is similar in length to those in **12** and **13**. The $SnPh_3$ ligand is positioned *cis* to the metal−metal bond, Sn(1)−Os-(1)−Pt(1) = 90.456(12)°, Os(1)−Sn(1) = 2.6540(4) Å. The osmium atom has only two terminal CO ligands.

The formation of **18** occurs by the addition of 1 equiv of PhC_2H to **12**. As with the addition of PhC_2H to **17**, this may also occur initially at the platinum atom which has only a 16 electron configuration in **12**. C−C coupling to the alkenyl ligand occurs, and a CO ligand is lost from the osmium atom when the second double bond from the diphenylbutadienyl ligand becomes bonded to the osmium atom; see Scheme 4. The platinum atom in **18** has a 16 electron configuration, and the osmium atom has 18 valence electrons. It is possible that **18** could add and couple yet another equivalent of PhC_2H to its butadienyl ligand, and a continuation of this process could lead to a PhC_2H polymer, but we have not investigated this yet.

Conclusions

We have shown in this work that an unsaturated Pt(PBu$^t_3$) group generated from the compound Pt(PBu$^t_3$)$_2$ by loss of a PBu$^t_3$ ligand can be added to the hydride complexes **10** and **11**, by forming an interaction to the hydrido ligand, the metal atom, and one of the CO ligands. It can facilitate insertion of the alkyne PhC_2H into the metal−hydrogen bond by providing a low lying empty orbital through which the alkyne can become coordinated and then be combined with the hydrido ligand. This is difficult for the hydride complexes **10** and **11** to do by themselves because both of these complexes have 18 electron configurations and are electronically saturated. We have been able to make both C−H and C−C bonds from **10** by using the Pt(PBu$^t_3$) activator.

Bimetallic cooperativity or synergism is an important feature of many heterometallic catalysts.[22] Such synergism may be

(21) (a) Clauss, A. D.; Tachikawa, M.; Shapley, J. R.; Pierpont, C. G. *Inorg. Chem.* **1981**, *20*, 1528−1533. (b) Shapley, J. R.; Richter, S. I.; Tachikawa, M.; Keister, J. B. *J. Organomet. Chem.* **1975**, *94*, C43−C46.

(22) (a) Adams, R. D. *J. Organomet. Chem.* **2000**, *600*, 1−6. (b) Thomas, J. M.; Johnson, B. F. G.; Raja, R.; Sankar, G.; Midgley, P. A. *Acc. Chem. Res.* **2003**, *36*, 20−30. (c) Hermans, S.; Raja, R.; Thomas, J. M.; Johnson, B. F. G.; Sankar, G.; Gleeson, D. *Angew. Chem., Int. Ed.* **2001**, *40*, 1211−1215. (d) Guczi, L.; Schay, Z.; Stefler, G.; Mizukami, *J. Molec. Catal.* **1999**, *141*, 177−185. (e) Sinfelt, J. H. *Bimetallic Catalysts. Discoveries, Concepts and Applications*; Wiley: New York, 1983. (f) Sinfelt, J. H. *Adv. Chem. Eng.* **1964**, *5*, 37−74. (g) Sinfelt, J. H. *Acc. Chem. Res.* **1977**, *10*, 15−20. Oh, S. H.; Carpenter, J. E. *J. Catal.* **1986**, *98*, 178−190. (h) Hogarth, M. P.; Ralph, T. R. *Platinum Met. Rev.* **2002**, *46*, 146−164. (i) Hogarth, M. P.; Hards, G. A. *Platinum Met. Rev.* **1996**, *40*, 150−159.

expressed by a variety of mechanisms, but few are understood in great detail. Here we have demonstrated a new example of bimetallic synergism in unusual detail and clarity.

Acknowledgment. This research was supported by the Office of Basic Energy Sciences of the U.S. Department of Energy under Grant No. DE-FG02-00ER14980. We thank STREM for donation of a sample of $Pt(PBu^t_3)_2$ and Johnson Matthey for a donation of K_2PtCl_4. We wish to thank Dr. Perry J. Pellechia for assistance with the variable temperature NMR spectra. Dedicated to the memory of F. Albert Cotton.

Supporting Information Available: CIF files for each of the structural analyses. This material is available free of charge via the Internet at http://pubs.acs.org.

JA070617H